

Synchrotron XRF Microprobe Analysis of Geological Samples: Influence of Size and Orientation of Single Mineral Grains[†]

M. O. Figueiredo,^{1*} M. T. Ramos,² T. Pereira da Silva,¹ M. J. Basto³ and P. Chevallier⁴

¹ Crystallography and Mineralogy Center, IICT, Alameda D. Afonso Henriques 41–4°, P-1000 Lisbon, Portugal

² Atomic Physics Center, University of Lisbon, Av. Gama Pinto 2, P-1699 Lisbon, Portugal

³ Mineralogy and Petrology Laboratories, IST, Av. Rovisco Pais 1, P-1096 Lisbon, Portugal

⁴ LURE, Centre Universitaire Paris-Sud, Bâtiment 209C, F-91405 Orsay, France

The results of a photon microprobe study on the influence of size and orientation of single mineral grains on geochemical data when analysing geological samples are presented. A large crystal of primary pegmatitic muscovite and an aggregate of small lamellar secondary lepidolite grains were analysed at various points. The primary synchrotron radiation beam orientation has a negligible effect upon geochemical data for tetrahedral and octahedral cations in both minerals. Conversely, the analytical results for the large interlayer cations are significantly more dispersed when the incident beam is parallel to the (001) plane of the crystal(s). Furthermore, the analysis of the sub-parallel aggregate of lepidolite minute crystals provided higher concentration figures for substituting large cations (particularly caesium) when the incoming beam was so oriented. Copyright © 1999 John Wiley & Sons, Ltd.

INTRODUCTION

The use of photon microprobes for the non-destructive *in situ* elemental analysis of single mineral grains has been most successful for the geochemical characterization of geological materials. However, some analytical difficulties and drawbacks have already been recognized either in relation to the bonding situation of the element to be analysed,^{1–5} viz. energy shifts and intensity variations of spectral lines plus the appearance of extra satellite lines, or in a strict dependence on the response function of the Si(Li) detector.^{6,7}

Bonding effects display a clear dependence on the mineral carrying the analyte. Indeed, the crystal structure constrains the population of chemical elements that may be incorporated by a given mineral, mainly due to crystal field effects related to the configuration of available structural sites. Accordingly, the geometrical diversity of sites that may be filled in a given mineral structure accounts for an increased range of geochemical substitutions and, consequently, for a greater complexity of the x-ray fluorescence spectrum corresponding to that mineral.

Additional disturbing features can be detected when analysing geological samples arising from the structural control of mineral chemistry in connection with the minute dimensions of the irradiated area, mainly due to the influence of size and orientation of single mineral grains.

Analytical potential hazards when using synchrotron radiation (SR) in a photon microprobe instrumental set-up (μ -SRXRF) are illustrated in the present study by the analysis of mica samples.

EXPERIMENTAL

The crystal chemistry of mica minerals is particularly suitable for studying the effect of grain size and crystallite orientation upon geochemical data as ascertained by μ -SRXRF. These minerals are light silicates with a layered crystal structure containing tetrahedral, octahedral and larger interstices with coordination number (CN) 12–9. Each type of site in primary micas is capable of hosting a specific cationic population and, therefore, the geochemistry of primary micas supplies valuable data concerning the chemistry of the growth medium. On the other hand, the surface of single grains in secondary micas provides active sites that may adsorb particles of minute dimensions, increasing the span of transported elements. Accordingly, mica minerals may display geochemical features arising from substitutional and from adsorptively retained trace elements.

The mica samples studied come from pegmatites in Mozambique, eastern Africa: primary muscovite, ideal chemical formula $\text{KAl}_2(\text{OH})_2[\text{AlSi}_3\text{O}_{10}]$, from Mt Dombe, Tete province, and lepidolite, ideally $\text{KLi}_2\text{Al}(\text{OH})_2[\text{Si}_4\text{O}_{10}]$, from Muiane pegmatite in Zambezia province. The crystal structures of these samples were previously checked by x-ray diffraction, both having the structure of polytype 2M₁. Lepidolite was therefore assumed to be secondary in origin as it does not display the polytype 2M₂, usual for primary lepidolites.

* Correspondence to: M. O. Figueiredo, Centro de Cristalografia e Mineralogia, IICT, Alameda D. Afonso Henriques 41–4°, P-1000 Lisbon, Portugal.

E-mail address: mof@mail.fct.unl.pt

[†] Presented at the European Conference on EDXRS, Bologna, Italy, 7–12 June 1998.

Contract/grant sponsor: European Union.

Two lamellar single crystals, one 20 times thicker than the other, of muscovite were analysed across the *a,b* or (001) plane at different points with the incident synchrotron beam inclined 45° to the surface, to check the chemical heterogeneity (zoning) of the crystal and the influence of thickness in homogeneous regions. Similarly, an aggregate of sub-parallel lepidolite lamellar minute grains (crystals) was analysed both parallel to and across the (001) plane.

SRXRF spectra were collected at the LURE (Laboratoire pour l'Utilisation du Rayonnement Electromagnétique) in Orsay, France, at the D15A experimental station of the DCI storage ring using the microprobe mounting equipped with a Si(Li) detector. A complete description of the instrumental set-up of the LURE microprobe may be found elsewhere.^{8,9}

The spectra were collected for 1000 sec with an excitation energy of 13.4 keV, the detector being placed at a distance of 3 cm from the sample. The area to be irradiated (0.03 mm²) was positioned with the aid of a laser beam using a computer-controlled micrometer stage. Peak assignment is based on the diagnostic lines: $K\alpha$ lines in the x-ray emission spectrum of elements with medium atomic number and $L\alpha$ for elements with $Z > 37$. Data handling and processing programs developed at the LURE were used in spectra deconvolution and analysis.^{10,11}

RESULTS

As expressed by the ideal chemical formula of the studied mica minerals, the common major elements are Si, Al and K, Li being the additional major component of lepidolite.

SRXRF data showed that the minor components Mn, Fe and Zn are present in both micas at different concentration levels: lepidolite is richer in manganese and zinc whereas muscovite is richer in iron. Other minor elements are Ga and Ge, the first much more represented in muscovite.

A large group of trace elements are also present in both minerals at variable levels: Ca, Ti, V, Cr, As, Rb, Zr, Nb, Mo, Cd, In, Cs, Ba, Ta, W and Tl. The last three heavy elements display relative proportions $W > Ta > Tl$ in muscovite and $Ta > Tl > W$ in lepidolite (see Fig. 1). Some LREE were also detected, namely La, Ce, Nd and Sm. As the experiments were performed in air, a few light elements that are probably present, such as fluorine and sodium, could not be observed.

The detected minor and trace elements differ in geochemical behaviour and a bulk evaluation of analytical data would mask important relationships and hinder useful conclusions. Therefore, these elements were first grouped according to the structural site that they will presumably occupy in mica structure, tetrahedral, octahedral and large sites, taking into account the geochemical trends generally accepted for each element. Accordingly, potassium in the interlayer sites may be partially replaced by large-radius, low-valency ions such as Rb^+ or by smaller monovalent (Na^+) or divalent (Ca^{2+}) ions in distorted interstices with lower coordination (CN 9–10). The larger cations Cs^+ and Ba^{2+} are also possible candidates to replace K^+ , particularly in lepidolites where the interlayer site is larger and less distorted (CN 12).

The tetrahedral sites, occupied by Si with minor Al, may accommodate ions with high formal valency and small radius such as Ga^{3+} , Ge^{4+} and As^{5+} . Other ions may also enter these interstices, such as Zn^{2+} or In^{3+} in lepidolite.

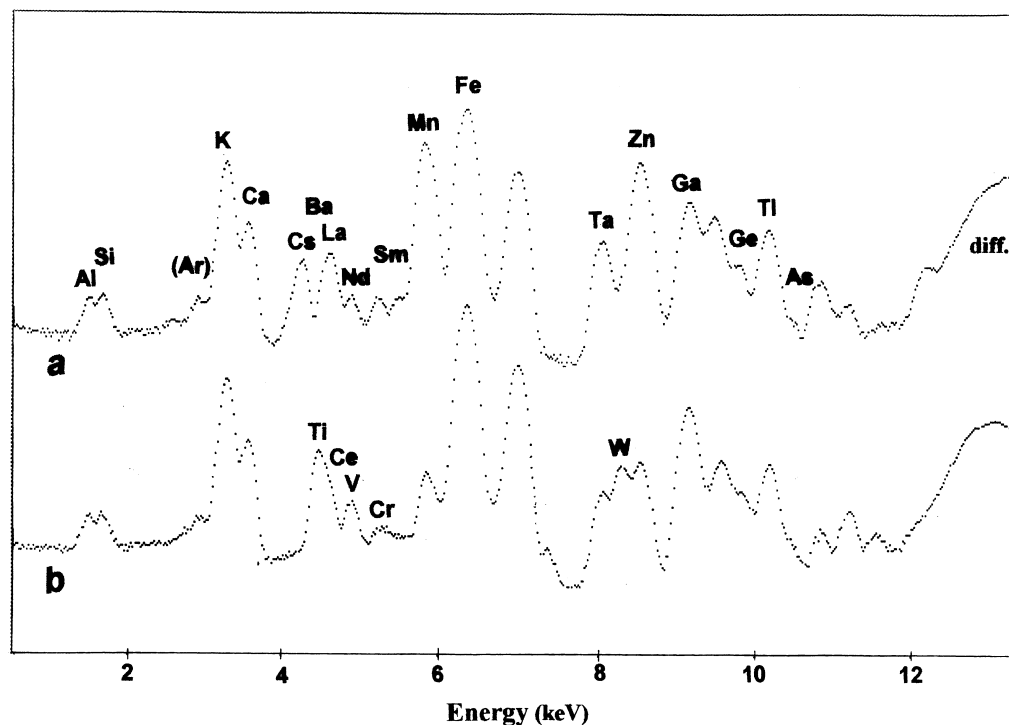


Figure 1. Illustrative examples of SRXRF spectra (semilog scale, intensity in arbitrary units) from (a) lepidolite and (b) muscovite. Only the diagnosis peaks are assigned, $K\alpha$ or $L\alpha$ depending on the atomic number of the element. Important chemical differences are apparent in the regions Cs–Ti–Ba–La–Ce–V–Nd–Cr–Sm and Ta–W–Zn.

The remaining elements behave essentially as octahedral cations replacing aluminum and/or lithium either as divalent (essentially Mn and the sub-trace element Cd), trivalent (Fe, Cr), tetravalent (Ti, Zr) or higher valency ions (Ta, W, Nb, Mo). The geochemical trend is uncertain for Tl once this element may behave as an octahedral trivalent cation or else as a large monovalent ion, in this case replacing potassium. The first tendency was assumed in view of the relatively high thallium content in both minerals.

The areas of the diagnostic peaks ($K\alpha$ or $L\alpha$ lines) corresponding to most representative elements within each group were summed and ratios calculated for the sums of peak area for major plus minor components assumed for each site, that is, K vs $(Ca + Cs + Ba)$ for large interlayer sites in lepidolite and K vs $(Ca + Ba)$ in muscovite (no Cs was detected); $(Al + Mn + Fe)$ vs $(W + Ta + Ti)$ for octahedral interstices and $(Al + Si + Zn)$ vs $(Ga + Ge)$ for tetrahedral positions in both minerals.

Graphical plots of calculated ratios for points analysed with the incident beam oriented across the basal (001) plane, labelled B, and along that plane, labelled L, in the aggregate of sub-parallel lepidolite grains are displayed in Figs 2–4. The dispersion of calculated ratios seems fortuitous for both tetrahedral (Fig. 2) and octahedral (Fig. 3) site populations. Conversely, the two data sets

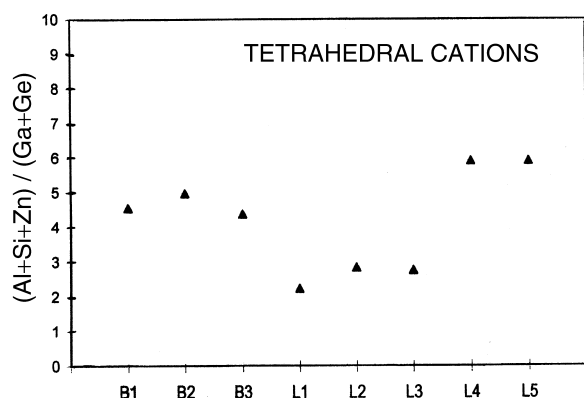


Figure 2. Graphical plot of calculated sums of peak area ratios $[(Al + Si + Zn)/(Ga + Ge)]$ for the aggregate of sub-parallel lepidolite grains/crystals. *B*, basal points, analysed with the incident SR beam oriented across the (001) plane of the crystals; *L*, lateral points, analysed with the beam oriented parallel to that plane.

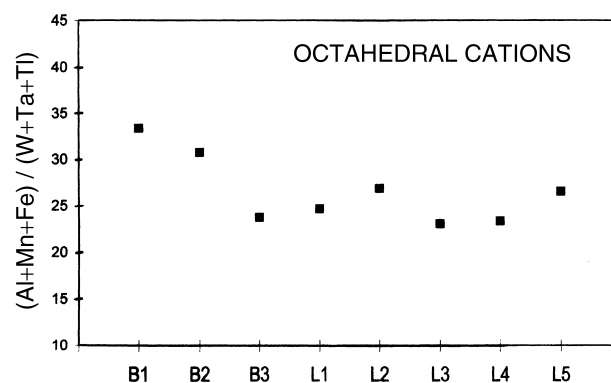


Figure 3. Plot of calculated peak area ratios $[(Al + Mn + Fe)/(W + Ta + Ti)]$ for lepidolite.

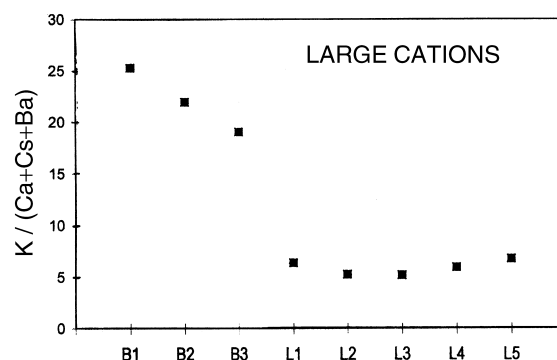


Figure 4. Plot of calculated peak area ratios $[K/(Ca + Cs + Ba)]$ for lepidolite.

B and *L* present clearly different numerical trends for the cationic population of the large site (Fig. 4).

The thick fragment of muscovite was visibly zoned, displaying a heterogeneous distribution of diadochic substitutions with a clear dependence on the surrounding chemistry of the medium during crystal growth. This was particularly apparent for the relative content of zinc in octahedral sites.

The analysis of the large-site cationic population also provided interesting results for which no immediate explanation could be found. Indeed, a significantly larger dispersion of calculated peak area ratios $[K/(Ca + Cs)]$ was obtained for the thick lamellar aggregate (T) compared with the very thin muscovite slice or single lamella (S), as illustrated by Fig. 5.

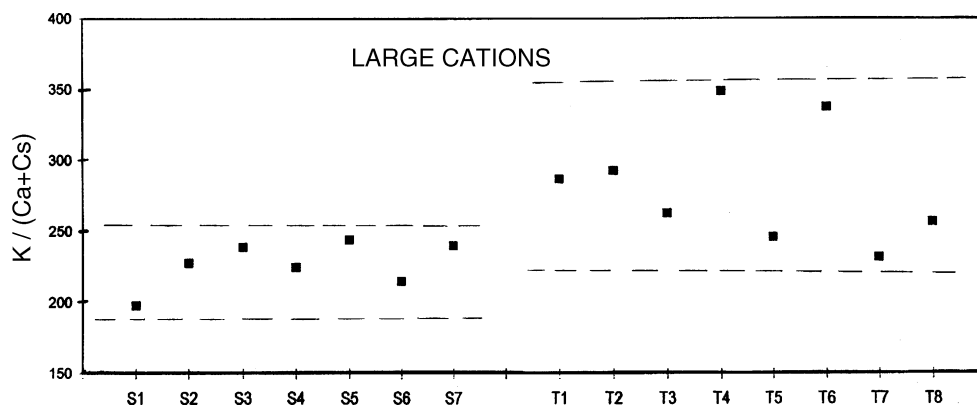


Figure 5. Plot of calculated peak area ratios $[K/(Ca + Cs)]$ for muscovite. *S*, single lamella; *T*, thick aggregate of lamellae.

CONCLUSIONS

The use of photon microprobes has enormously enhanced analytical capabilities, particularly for complex materials such as most geological samples. This technique has further made possible the mapping of elements in the analysed sample. Conversely, the reduced irradiated area (0.03 mm²) has significantly diminished the bulk representativity of analytical data, a feature sufficiently recognized that must be taken into account when using isolated mineral grains for geochemical analysis.

The present μ -SRXRF study has thrown some light upon the importance of considering the geochemical role of each element in parallel with the crystal chemical characteristics of constituent minerals in geological materials.

In fact, it becomes explicit from Fig. 4 that some trace elements, usually considered to be replacing potassium by diadochy, may be in part concentrated on active sites at the lateral surface of single grains/crystals in secondary micas. When so much is being written on 'invisible' elements, these results also emphasize the need for further studying the effects of adsorbed and occluded nanoparticles on geochemical results obtained by photon microprobe techniques.

Acknowledgements

The authors gratefully acknowledge the financial support of the European Union through the HCM Programme for conducting the experimental work. The samples were kindly supplied by Professor Fung Dai Kin of the Eduardo Mondlane University, Maputo, Mozambique.

REFERENCES

1. C. V. Raghavaiah, N. Venkateswara Rao, G. Sree Krishna Murthy, M. V. S. Chandrasekhar Rao, S. Bhuloka Reddy and D. L. Sastry, *X-Ray Spectrom.* **21**, 239 (1992).
2. G. Peng, F. M. F. deGrrot, K. Hamalainen, J. A. Moore, X.-Wang, M. M. Grush, J. B. Hastings, D. P. Siddons, W. H. Armstrong, O. C. Mullins and S. P. Cramer, *J. Am. Chem. Soc.* **116**, 2914 (1994).
3. J. Kawai, T. Nakajima, T. Inoue, H. Adachi, M. Yamaguchi, K. Maeda and S. Yabuki, *Analyst* **119**, 601 (1994).
4. Y. Tamaki, *X-Ray Spectrom.* **24**, 235 (1995).
5. L. Rebohle, U. Lehnert and G. Zschornack, *X-Ray Spectrom.* **25**, 295 (1996).
6. N. P.-O. Homman and P. Kristiansson, *X-Ray Spectrom.* **25**, 66 (1996).
7. J. L. Campbell, J. A. Maxwell, T. Papp and G. White, *X-ray Spectrom.* **26**, 223 (1997).
8. P. Chevallier, P. Dhez, F. Legrand, A. Ekro, Yu. Agafonov, L. A. Pachenko and A. Yakshin, *J. Trace Microprobe Tech.* **14**, 517 (1996).
9. P. Chevallier, P. Dhez, A. Erko, A. Firsov, F. Legrand and P. Populus, *Nucl. Instrum. Methods Phys. Res. B* **113**, 122 (1996).
10. I. Brissaud, J. X. Wang and P. Chevallier, *J. Radioanal. Nucl. Chem.* **131**, 399 (1989).
11. K. Abbas, PhD Thesis, Université Paris VI (1991).